JOURNAL OF AIRCRAFT
Vol. 47, No. 6, November–December 2010

Airfoil Lift Augmentation at Low Reynolds Number

Lance W. Traub* and Adrian Akerson†
Embry–Riddle Aeronautical University, Prescott, Arizona 86301

DOI: 10.2514/1.C000326

A low-speed wind-tunnel investigation was undertaken to explore the behavior of trailing-edge flow effectors on the performance of a S8036 airfoil. Gurney flaps, as well as conventional trailing-edge flaps, were explored at $Re = 40,000$, 60,000, and 80,000. The effects of Gurney flap length, as well as trailing-edge flap length and deflection angle, were studied. Performance characterization encompassed force balance and pressure measurements. Examination of the results showed that both types of flaps are capable of significantly increasing not only the maximum lift coefficient, but also the range and endurance parameters. For the geometries explored, both the Gurney and trailing-edge flap showed similar levels of lift augmentation; however, the trailing-edge flaps generally showed larger relative increments in the lift-to-drag ratio and endurance parameter than the Gurney flaps.

Introduction

ECONOMIC viability, mission flexibility, and expanding application have thrust the research focus devoted to small-scale unmanned aerial vehicles (UAVs) from the domain of radio-control hobbyists to the mainstream research community. UAVs may range in size from the so-called micro, with a somewhat arbitrary span requirement of 6 in. or less, to large-sized vehicles, such as the Predator B, weighing in at 10,000 lb. Smaller UAVs may find application in reconnaissance missions, where the ability of a local commander to rapidly see "over the hill" is invaluable. However, aerodynamic design at low Re that, depending on the focus, may be considered as less than 200,000, becomes complicated. Pioneering studies and reviews by Mueller [1,2], Perry and Mueller [3], Lissaman [4], and others greatly expanded the understanding of these low-Reynolds-number flows. The production of high lift coefficients, which may be of value for pinpoint loitering, reduced stall speed, landing and taking off, or potentially increasing endurance, is severely hampered at low Re.

Low-Reynolds-number flows are typically dominated by the presence of large extents of laminar flow [4]. This limits the pressure recovery capabilities of the boundary layer and generally necessitates the requirement to promote transition to accomplish recovery without large-scale flow separation. Unless the Re is very low (less than 75,000), transition is naturally accomplished through the formation of a laminar transitional bubble [1,4]. Suppression of transition (due to very low Re) usually manifests in large-scale laminar separation. A focused research effort by the community has clarified the behavior of these bubbles [2,4,5]. While the bubble results in transition, it does cause a drag increase, as the momentum thickness of the reattached boundary layer is greater than through an attached flow transition process. Unless very large, the bubbles generally do not impact the developed lift significantly [4].

At high Reynolds numbers, lift augmentation is usually accomplished by employing a trailing-edge flow effecter, such as a trailing-edge flap [6]. Through increased camber, flaps generally shift the zero-lift angle of attack (AOA) in the negative direction without a significant change of the lift-curve slope. The maximum lift coefficient is increased, but stall typically occurs at lower incidence. Depending on the subtleties of the design and the deflection angle of the flap, drag is usually increased. Few studies appear in the literature that investigate trailing-edge flaps at low Re. A study by Perry and Mueller [3] on a Wortmann FX63-137 airfoil, with both leading-edge and trailing-edge flaps at $Re = 100,000$ and 150,000, showed that trailing-edge flaps could increase the maximum lift coefficient but degraded both the lift-to-drag ratio L/D and the endurance parameter $C_l^{3/2}/C_d$ (where L and C_l are lift and lift coefficient, respectively, and D and C_d are drag and drag coefficient, respectively) due to a significant increase in the minimum drag coefficient.

Recent studies [7–9] have shown the potential of the Gurney flap to significantly augment lift, coupled with unparalleled simplicity of design and structure. The flap, in essence a small thin element attached perpendicular to the trailing edge on the pressure side, may increase lift with a marginal drag penalty if located within the lower-surface boundary layer [7]. Consequently, an increase in the lift-to-drag ratio may be realized. Gurney flaps function in a manner dissimilar to conventional trailing-edge flaps. Pressure traces around a Gurney-flap-equipped wing show an apparent violation of the Kutta condition, such that final pressure recovery occurs in the wake. Increased base suction due to flow entrainment caused by the formation of a von Karman vortex street [10] and augmented lower-surface recompression are causal in the finite trailing-edge pressure difference. Thinning of the lower-surface boundary layer with incidence coupled with reduced upper-surface pressure recovery demands [9] (hence, a potential lower displacement thickness and effective airfoil decambering), also causes an increase in the lift-curve slope in conjunction with a negative shift in the zero-lift angle. Asymmetric boundary-layer growth as the cause of lift-curve slope increase is also supported by data for so-called T strips (in essence, a symmetrical upper and lower Gurney flap implementation). Reported data [11] show that the T strip displays little effect on the measured lift at low incidence. With increasing incidence, the T strip shows a lift-curve slope increase, reflective of the thinning of the lower-surface boundary layer and thickening of the upper-surface boundary layer.

Efforts to reduce the drag penalty that are sometimes associated with Gurney flaps have generally focused on disturbing the organized wake structure observed behind these flaps. A study by Meyer et al. [12] and a survey by Mayda et al. [13] have shown that the introduction of streamwise jets (porous or slotted/serrated flap geometry) can aid in the destruction of the absolute instability. However, the reduction in drag is also accompanied by a loss of lift, yielding this form of drag abatement not entirely satisfactory, depending on the application. Porous [14] Gurney flaps show a similar result. Inclining the flap, such that it is not at 90 deg but 45 deg to the lower surface, has been shown to reduce drag while maintaining lift augmentation if the projected flap height is conserved [15].

Consequently, this paper details a systematic effort to increase the available database on the effect of lift-augmentation devices for low

Received 22 February 2010; revision received 3 May 2010; accepted for publication 3 May 2010.

*Associate Professor, Aerospace and Mechanical Engineering Department. Member AIAA.

†Undergraduate Student, Aerospace and Mechanical Engineering Department.

Table 1 Pressure port locations

$(x/c)_u$	0	0.015	0.05	0.075	0.1	0.125	0.15	0.175	0.2	0.25	0.3	0.35	0.4	0.45	0.5	0.55	0.6	0.7	0.8	0.9
$(x/c)_l$	0	0.0175	0.1	0.15	0.2	0.3	0.4	0.5	0.6	0.7	0.8	—	—	—	—	—	—	—	—	—

Re applications. Trailing-edge flaps, as well as Gurney flaps, are investigated. Various trailing-edge-flap setting angles and lengths are evaluated. For the Gurney flaps, the effect of flap length is examined. Performance characterization includes force balance, pressure measurement, and surface flow visualization.

Equipment and Procedure

Wind-tunnel tests were conducted in Embry–Riddle University's 1 by 1 ft open-return facility. This wind tunnel has a measured turbulence intensity of 0.5% and jet uniformity within 1% in the core. The wall boundary layer is approximately 5 mm thick. Force measurements were taken using an in-house designed and manufactured low-range platform balance. The balance has a maximum range of 43 N and a demonstrated accuracy, resolution, and repeatability of 0.0098 N. Angle setting ability is within 0.1 deg. Tests were conducted at Reynolds numbers of 40,000, 60,000, and 80,000. A computer-controlled acquisition system was written for this balance using LabVIEW 8.2. All signals were low-pass-filtered and averaged such that each presented data point represents an average of a thousand readings.

Three wings were used in the present study. They were designed using CATIA software and then rapid-prototyped using Embry–Riddle's rapid prototyping facilities, yielding acrylonitrile butadiene styrene plastic wing representations. The section used was a S8036 with a thickness of 16%. The profile was chosen due to its effective performance at low *Re* numbers. The wings had a chord of 100 mm. One wing served for Gurney flap testing, another was designed to accommodate the attachment of plain flaps, and the last was pressure-tapped (this wing does not have the facility to evaluate deflected trailing-edge flaps). The wings spanned the tunnel to facilitate two-dimensional flow and may thus be considered as airfoils. For the force balance testing cases, the gap between the model and wall was measured as less than 0.5 mm. The pressure tappings were located at 40% of the span and were inclined at 30 deg to avoid potentially transitioning the boundary layer (see Fig. 1). Port set B was used in this study. A total of 30 taps were used: 20 on the upper surface and 10 on the lower surface. The tubing used for the ports located from the nose to 20% c had an internal diameter of 0.25 mm. Tubing located aft of this location had an internal diameter of 0.5 mm. Smaller tubing was not used, due to extremely slow response time and the high probability of tapping obstruction. Great care was taken to ensure that the taps were clean and did not protrude from the surface. The taps were formed by passing Tygon tubing of the appropriate internal diameter through a preformed location hole in the rapid-prototyped wing surface. The tubing was then bonded in place on the inside of the wing and cut to length, using a thin blade held parallel to the surface. This method resulted in cleanly formed pressure taps that were flush with the surface. This was checked both tactilely and using a 10x magnification loupe. Locations of the pressure taps are given in Table 1, where x and c correspond to locations along the chord length, respectively. The upper and lower surfaces correspond to u and l, respectively.

The Gurney flap configurations may be seen in Fig. 1. Flaps with lengths of 0.8, 3, and 4.5% of the chord were evaluated. Additionally, an inclined flap (at 45 deg) with a projected height of 3.9% chord was tested. The Gurney flaps (formed from thin brass sheet) were attached to the wing using thin double-sided tape. Conventional plain trailing-edge flaps were also investigated. Ten- and 20%-long flaps were manufactured, with deflection angles of 0, 10, 20, and 30 deg.

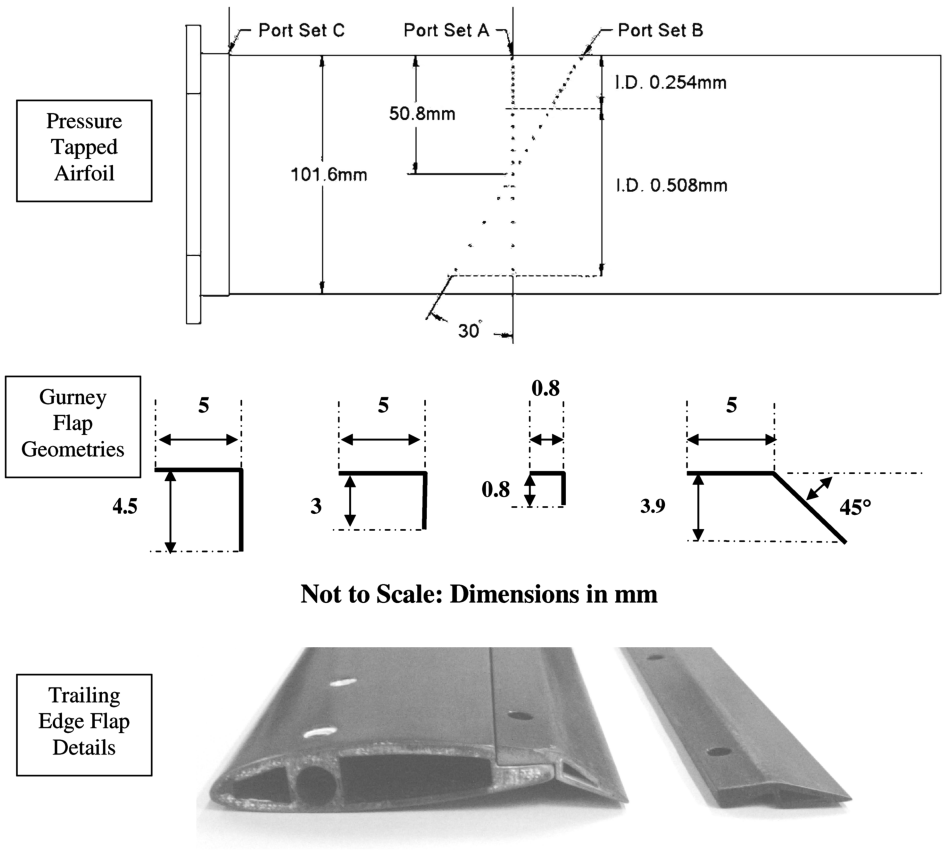

Fig. 1 Wind-tunnel model details showing Gurney flap geometries, flap attachment, and pressure port layout.

Figure 1 shows an example. The flaps were attached to the main wing panel, using small screws. Any gaps present were filled, using clay, and smoothed over. The 0 deg flap case was used as the representative clean airfoil case for the trailing-edge flap investigation.

Pressures were measured using an electronic pressure scanner. The scanner contains 30 independent temperature-compensated differential pressure transducers. An interface was written in Visual Basic to process and record the measured pressures. The pressure transducer outputs were digitized, using a 32-channel 16-bit National Instruments external universal serial bus analog-to-digital converter board. The board allows scanning of the pressures at up to 250, 000 reading/s. All presented pressures are the average of 1000 readings. Calibration of the scanner was performed using a FlowKinetics LLC FKT 1DP1A-SV pressure/flow meter. The FKT meter was calibrated against a deadweight primary standard and was within its calibration specifications. Comparison with the standard showed accuracy of better than 0.5 Pa. Calibration and comparison of the scanner with the FKT meter showed measured pressure agreement within 0.8 Pa for all 30 of the transducers. The tunnel freestream velocity was measured using a FlowKinetics FKT 2DP1A-C meter. This meter measures atmospheric pressure, temperature, and relative humidity, all of which are used to compute the density used in the velocity calculation. Meter accuracy is specified by the manufacturer as better than 0.1%. Because of the comparative nature of the tests and questionable validity at very low Re, wall corrections were not applied. Force coefficients were nondimensionalized by the projected area of the wing and any extension added by the Gurney flaps, where applicable.

Results and Discussion

In the following discussion, the unmodified airfoil without any flap addition or deflection is designated as the clean airfoil. Note that the clean airfoil for the trailing-edge flap tests was that with a flap attached with zero deflection; consequently there are two clean airfoil data sets (one for the Gurney flaps and one for the trailing-edge flaps). This approach was adopted as, at these low Re, small differences in the finish or geometry after preparation of the model can significantly affect the presented data. At low Re numbers, data fidelity is a major concern. Consequently, Fig. 2 shows repeated data runs for the 45 deg inclination Gurney flap configuration; the lift plot shows data for both increasing and decreasing incidence for both runs. Repeated measurements during the test also facilitated the calculation of uncertainty intervals, as indicated by the legend size on the figure. As may be seen, data reliability appears good.

Gurney Flaps

The effect of the Reynolds number on the clean airfoil and the airfoil with the 4.5% chord high (where the percentage is referenced to the chord) Gurney flap is explored in Fig. 3. Effects of hysteresis are indicated by the dotted-line types for the series. At $Re = 40,000$, the Gurney flap significantly increases the lift coefficient, effected through a large increase in the lift-curve slope. Surface pressure measurements for these conditions are presented in Fig. 4a. At $Re = 40,000$, pressure traces indicate large-scale flow separation for the clean airfoil upper surface combined with extents of suction from the lower surface (i.e., negative pressures) for the AOAs shown. The enhanced lift of the flap is seen to be due to both greater upper-surface suction as well as lower-surface compression. The appearance of a laminar transitional bubble is seen for the Gurney flap at 8 deg incidence. Although the small model geometry precluded tapping close to the trailing edge, the behavior of the Gurney pressure traces suggests a likely finite pressure difference at the trailing edge, as is well documented for these flaps. At this Re, hystereses is not shown to be significant, most likely a consequence of the stability of the boundary/shear layer (Fig. 3) and lack of bubble formation for the clean airfoil. The data suggest that the clean airfoil experiences laminar flow only, while the Gurney flap addition can lead to transition though a bubble. This may be due to the increased adverse pressure gradient with the flap promoting boundary-layer disturbance growth such that transition is achieved in the shear layer.

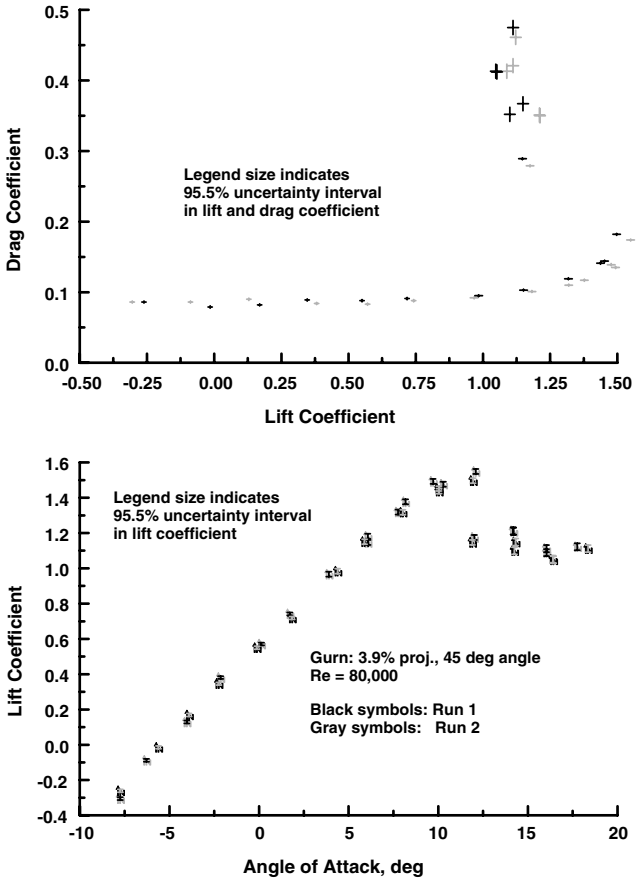

Fig. 2 Data repeatability and uncertainty.

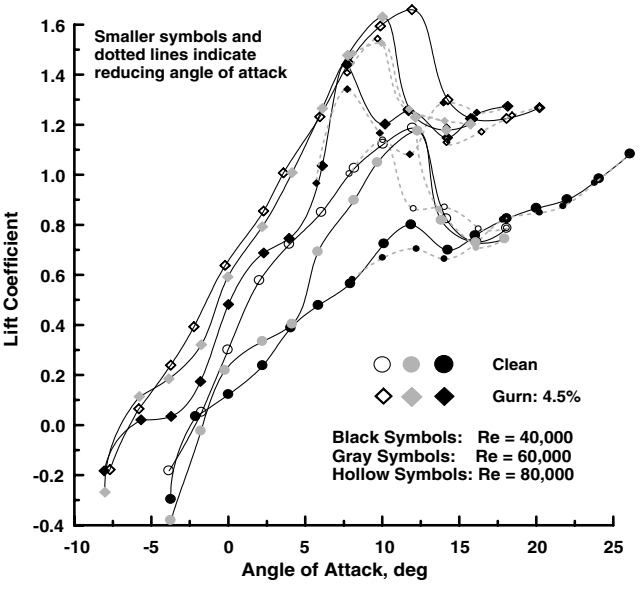

Fig. 3 Effect of Re on measured lift coefficient.

At $Re = 60,000$, the clean airfoil shows significant improvement in lift production and the appearance of a distinct stall. Pressure traces at this Reynolds number (see Fig. 4b) show an increase in peak suction and clearly visible transition, with bubble closure for both cases. The Gurney flap is seen to show enhanced suction over the entire upper surface and greater compression on the lower surface for the traces presented. As shown in Fig. 3, the effect of the flap may be identified as a zero-lift AOA shift and an increase in the lift-curve slope.

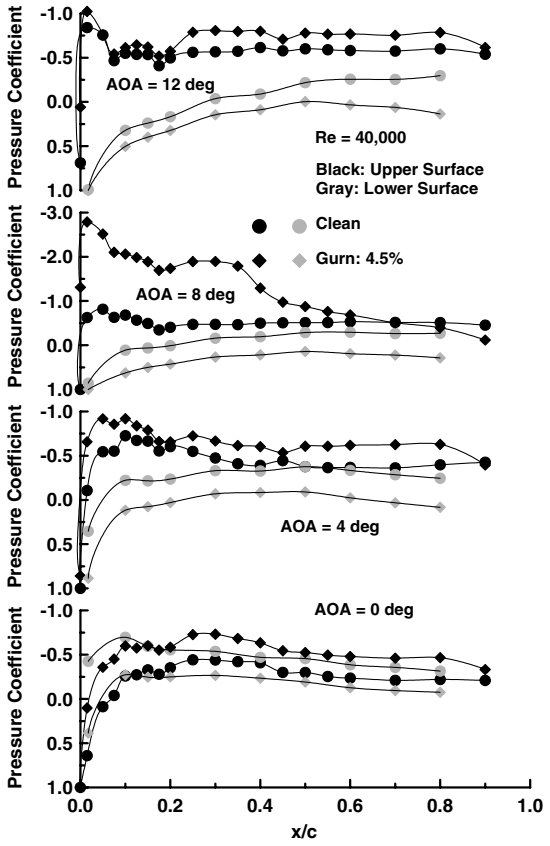

a)

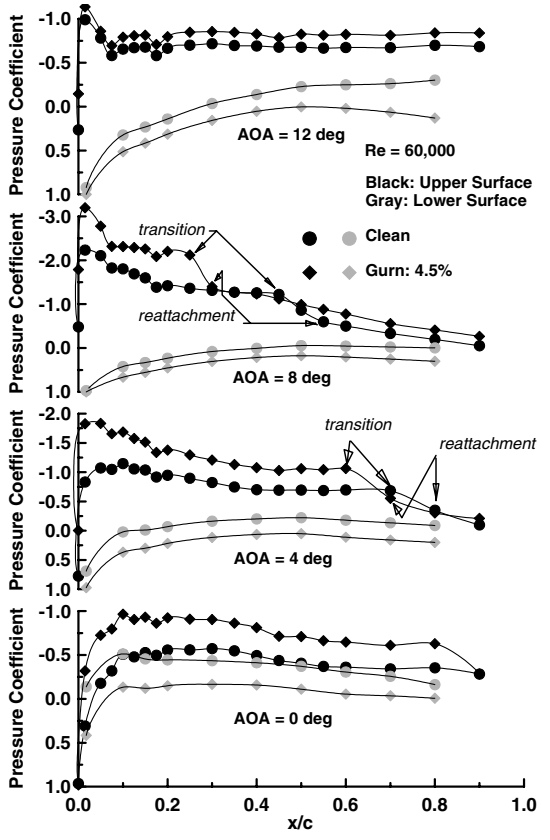

b)

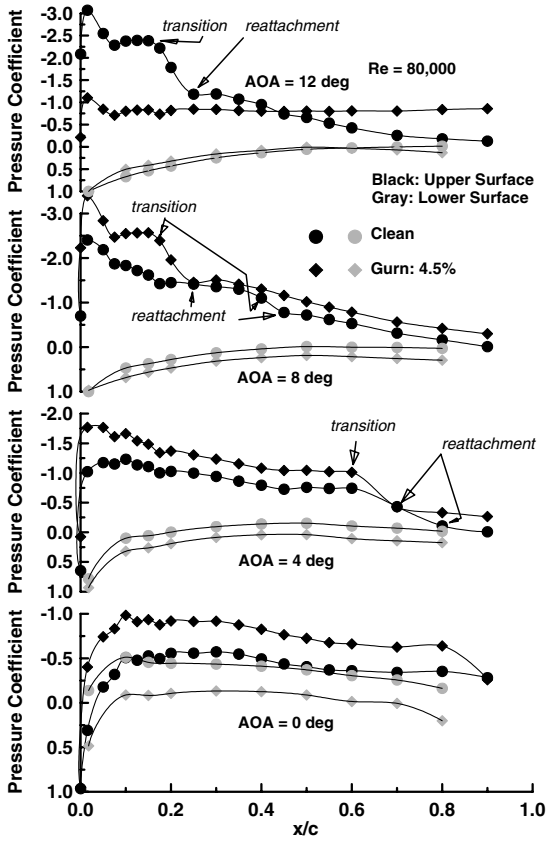

c)

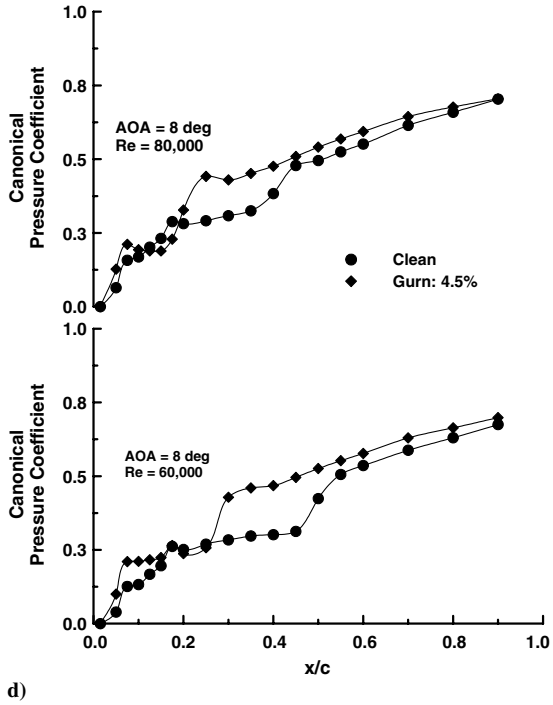

d)

Fig. 4 Effect of Gurney flap on surface pressure traces and skin friction topology: a) $Re = 40,000$, b) $Re = 60,000$, and c) $Re = 80,000$, and d) canonical pressure distribution.

The increase in the Re from 40,000 to 60,000 shows an improvement in the performance of the Gurney flap but to a lesser extent than that seen for the clean airfoil. Hysteresis is seen to be marginal for both airfoil configurations.

At $Re = 80,000$, the trend of improved lifting performance with increasing Re is evident; however, the relative lift improvement increment diminishes as the Re increases (Fig. 3). This is especially true for the Gurney flaps but is also evident for the clean airfoil. For the Re range presented, increasing the Reynolds number increases the stall angle (by approximately 2 deg for each 20,000 Re increment) and maximum lift coefficient of the Gurney-equipped airfoil. For the clean airfoil, the change in Re does not appear to affect the apparent stall angle, only the lift magnitude. Force balance data for the flapped configuration ($Re = 80,000$) show stall at a similar incidence to the clean airfoil, at approximately 12 deg. As seen in Figs. 4a–4c, the Gurney flap increases the velocity at the upper-surface trailing edge (so-called dumping velocity) reflected in a reduction in the surface pressure. This generally leads to reduced pressure recovery demands in the trailing-edge region; thus, an increase in overall upper-surface loading does not come at the expense of a lower stall angle, as is common for conventional trailing-edge flaps. However, the pressure trace shown in Fig. 4c for this incidence does not correlate with the lift shown in Fig. 3, where the maximum lift coefficient is indicated at this incidence (12 deg) for the Gurney. As shown, at 12 deg, the clean airfoil shows evidence of a suction peak and bubble, while the Gurney-equipped airfoil displays massive upper-surface separation. The disparity may be a consequence of small differences in the set incidence, as this angle is on the verge of stall. Hysteresis for both configurations appears to increase with Re, with the size of the loops (primarily clockwise in direction) enlarging, especially at $Re = 80,000$ (Fig. 3). The loop size appears larger for the Gurney-equipped airfoil in terms of lift coefficient excursion magnitudes.

Examination of Fig. 4 shows bubble behavior consistent with that reported in the literature [5], although more evident at $Re = 60,000$ and 80,000. Increasing incidence shows a forward movement of the bubble; however, for a given incidence, Re does not appear to significantly affect the separation location. This may be expected, as separation behavior is dominated by the shape of the pressure recovery region, which shows little variation with Re (see, specifically, Figs. 4b and 4c). The bubble length contracts moderately with incidence. This is primarily due to a shortening of the transition region of the bubble and, to a lesser extent, a shortening of the laminar bubble extent. For a given incidence, increasing the Re appears to contract the bubble (where clearly identifiable) (compare Figs. 4b and 4c; traces for the Gurney flap at 8 deg incidence). This appears to be due to an earlier onset of transition of the bounding free shear layer. As shear layers are highly receptive to disturbances, and an increase in Re increases the growth rate and range of frequencies that may amplify, this is not unexpected [16]. Bubble length appears similar for the clean and flapped airfoil for AOA = 0 and 4 deg (Figs. 4b and 4c). For 8 deg incidence (Figs. 4b and 4c), the flapped airfoil shows a shorter bubble than the clean airfoil geometry (verified through surface flow visualization). This may be caused by the higher pressure recovery demands aft of the suction peak (and, thus, potentially greater shear layer disturbance growth), with flap addition inducing earlier transition. It should be noted that the low AR of many small UAVs leads to highly three-dimensional flow that may significantly alter the separation and reattachment locations described previously.

Figure 4d presents pressure traces for the clean and flapped airfoil (4.5% chord Gurney) presented in canonical form. The canonical pressure distribution Cp_{canon} may be determined from traditional pressure coefficients (Cp, referenced to freestream static and dynamic pressure), using

$$Cp_{\text{canon}} = 1 - \frac{(1 - Cp)}{(1 - Cp_{\min})} \tag{1}$$

where $Cp_{\min}$ is the minimum pressure recorded in the trace. In essence, the canonical pressure distribution references the measured pressure to the minimum measured over the surface and the dynamic pressure associated with that minimum pressure. The canonical distribution is of value in interpreting and comparing boundary-layer behavior [17]. A coefficient of 1 represents stagnation–full-pressure recovery, and 0 represents the suction peak. As noted before, unlike conventional trailing-edge flaps, the Gurney flap does not reduce the stall AOA when compared with the clean airfoil at $Re = 80,000$, but it does at 60,000 (see Fig. 3). Using the Stratford criterion [18] for boundary-layer separation allows interpretation of the behavior of the canonical pressure distribution and its likely implications regarding the potential of the boundary layer to separate. Separation is dependent on both the canonical pressure gradient (an indicator of the local retarding force), as well as the magnitude of the canonical pressure (integral of the gradient and thus an indicator of the total retarding force since the start of pressure recovery) [18]. Consequently, a large gradient with a low magnitude of canonical pressure may yield a boundary layer resistant to separation. As shown in Fig. 4d, at $Re = 60,000$, the Gurney and clean airfoil show similar gradients near the trailing edge, but the canonical pressure magnitude is higher for the Gurney, suggesting that its boundary layer may be closer to separation, consistent with the earlier stall noted in Fig. 3. Increasing $Re(=80,000)$ indicates similar pressure magnitude and slope near the trailing edge, signifying similar separation resistance and, thus, stall onset in agreement with the presented data sets in Fig. 3.

Effects of the 4.5% chord Gurney flap at $Re = 40,000$ on the measured drag, range and endurance parameters are presented in Fig. 5. As may be seen, the addition of the flap (even at a size considered at the upper end of Gurney length) does not appear to markedly increase the minimum drag coefficient (Cd min). This may be due to the thick boundary associated with ultralow Reynolds

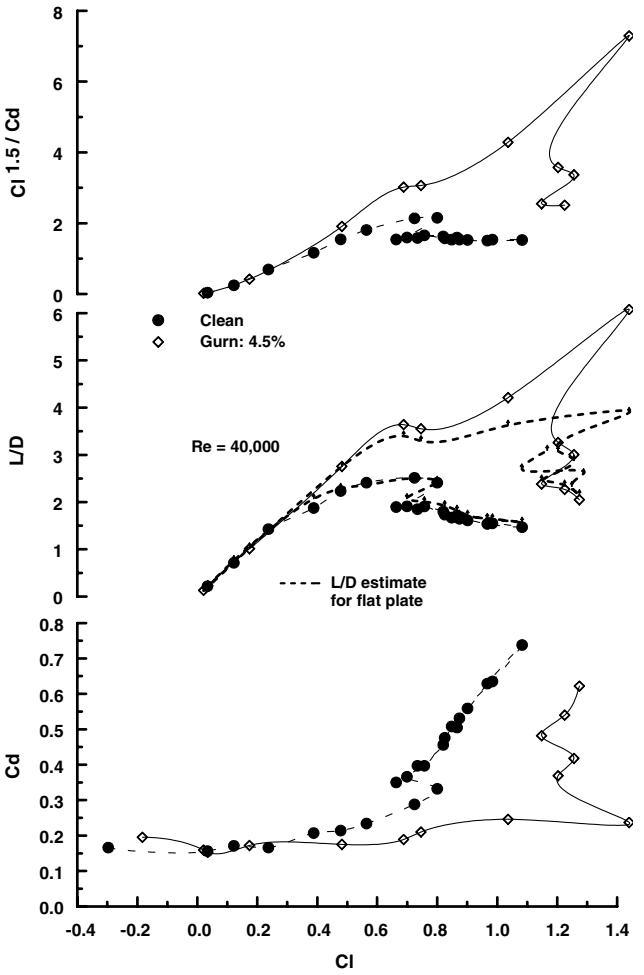

Fig. 5 Effect of Gurney flap on range and endurance parameters and the drag coefficient.

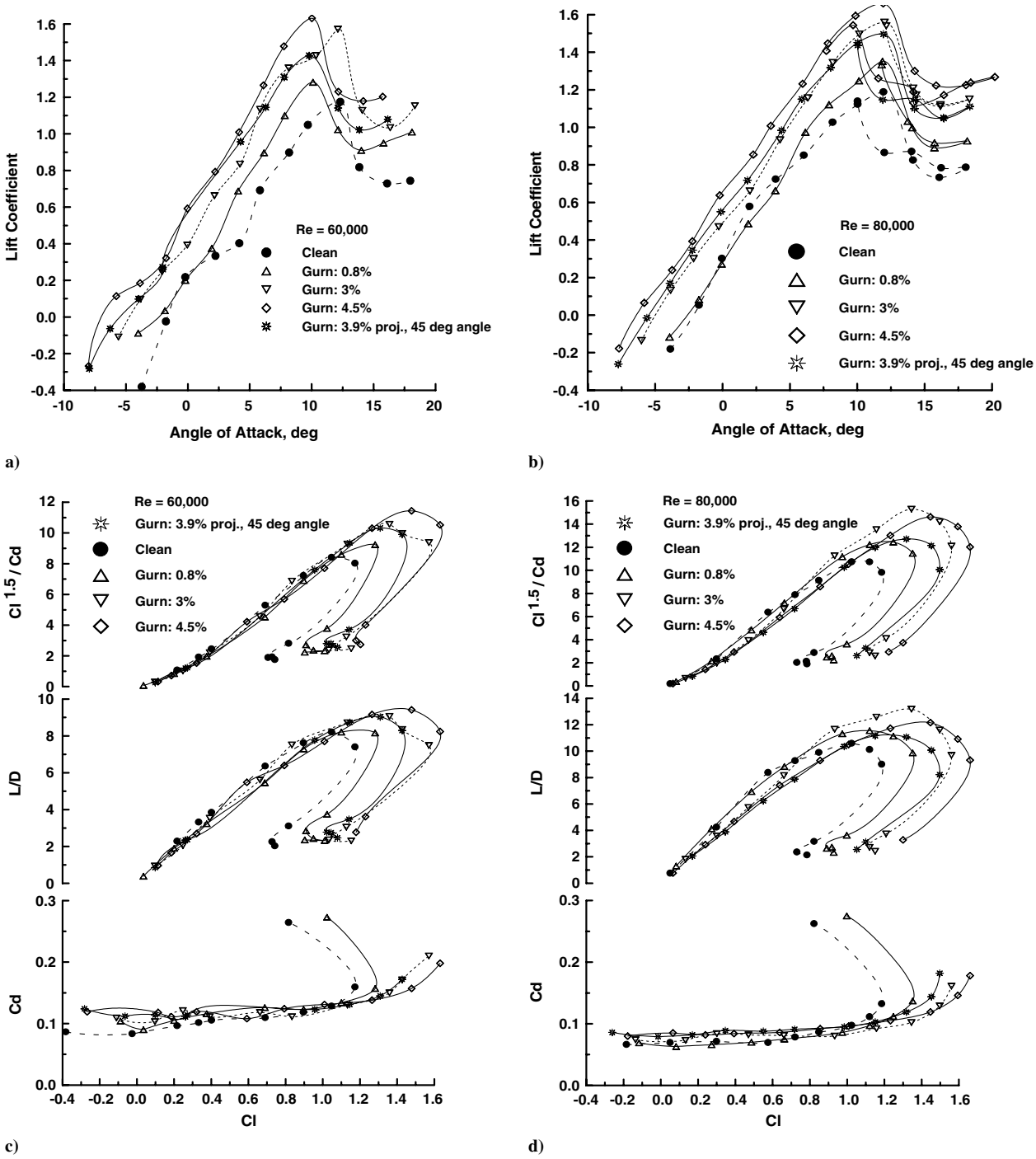

Fig. 6 Effect of Re and Gurney flap height on the measured lift coefficient and drag-based parameters: a) $Re = 60,000$, b) $Re = 80,000$, c) $Re = 60,000$, and d) $Re = 80,000$.

numbers. An Xfoil[‡] simulation for the clean airfoil at $Re = 40,000$ shows a lower-surface boundary-layer thickness of approximately 3.2% chord; consequently, in the minimum drag regime, most of the flap is imbedded within the boundary layer. The data indicate that, from moderate $Cl(>0.3)$, the addition of the flap significantly improves both the lift-to-drag ratio L/D (range parameter) and $Cl^{1.5}/Cd$ (endurance parameter). The large extents of flow separation at this Re render the airfoil (particularly, the clean geometry) highly inefficient. Included in the plot is an estimate of the L/D ratio for a flat plate, such that $\{L/D = Cl/(Cd\min + Cl\tan(\alpha)\}$. As may be seen, this estimate shows close accord with the clean airfoil and agreement with the flapped airfoil for $Cl < 0.4$. Consequently, the clean airfoil at this Re behaves essentially as a thin flat plate. At higher lift coefficients, it appears that the airfoil with the Gurney flap produces some leading-edge suction, as may be inferred from the appearance of a notable suction peak, as displayed in Fig. 4a.

Figure 6 presents a summary of the effects of Gurney flap height on the longitudinal performance parameters for $Re = 60,000$ and 80,000. At both Re, increasing flap length shows an increase in lift production, which is reflected primarily in a negative shift in the zero-lift AOA without a clearly identifiable change in lift-curve slope (Figs. 6a and 6b). At $Re = 60,000$, the lift peak for the flapped configurations occurs at approximately a 2 deg lower incidence than the clean airfoil. At $Re = 80,000$, all the configurations appear to stall at 12 deg (within the limitations of the AOA resolution). The maximum recorded lift coefficients increase slightly for $Re =$

[‡]Details available online at http://web.mit.edu/drela/Public/web/xfoil/ [accessed 10 January 2010].

80,000 when compared with 60,000 for respective configurations. Hysteresis loops are included for $Re = 80,000$; $Re = 60,000$ showed similar trends but were omitted for image clarity. As may be seen, the clean airfoil shows a clear hystereses loop with both anticlockwise (between 18 and 14 deg) and clockwise (between 14 and 10 deg) constituents. Typically, a clockwise hystereses loop forms if a transition bubble appears at moderate incidence, such that a relatively high maximum lift is produced [2]. A counterclockwise bubble may exist if flow separation occurs at low incidence, without shear layer transition or reattachment. At higher AOAs, shear layer transition results in turbulent attachment with an increase in lift, which is then maintained as the airfoil incidence reduces. The flapped airfoil also shows the presence of hystereses loops, where increasing flap height (within the range evaluated) enlarges the magnitude of the lift excursion traced by the loop (Fig. 6b). The 3% chord flap did not appear to show a significant loop; the reason for this was not established, but it is not considered to be typically representative.

Figures 6c and 6d, present the effect of Re and Gurney flap length on measured drag-based parameters. The attachment of the Gurney flaps is reflected in a drag coefficient increase for most data sets. In all instances, up to a lift coefficient of 0.8, the flap addition does not improve L/D and may degrade it (more pronounced at $Re=$ 80,000). The significant increase in the maximum lift coefficient with the Gurney is also reflected in a considerable increase in both the L/D and $Cl^{1.5}/Cd$ maximum. A flap length of 4.5% chord shows the highest range and endurance parameters at $Re = 60,000$, while at $Re = 80,000$, maximums are given by the 3% chord flap. This may be reflective of the thinning of the boundary layer with Re, yielding the 4.5% chord flap excessively high at $Re = 80,000$. The 45 deg inclined flap does not appear to show any particular advantage in terms of drag reduction and yields a performance comparable to the 3% chord Gurney at $Re = 60,000$ and somewhat inferior to this flap at $Re = 80,000$. Numerical values summarizing the effect of Re and flap length are presented in Table 2. As shown, the flaps significantly increase L/D (up to 24.6% for the 3%-long Gurney flap at $Re = 80,000$) and $Cl^{1.5}/Cd$ (42.8% increase for the 3%-long Gurney at $Re = 80,000$), with augmentation increasing slightly with Re. Note that the flap lengths for maximum performance enhancement (within the range tested) are significantly greater than the 1–2% chord commonly cited as optimal: a consequence of the thick boundary layers associated with low Re flows.

The effect of Gurney flaps has been shown to correlate with the square root of the flap length [19], a dependency demonstrated theoretically in [20] based upon thin airfoil theory. Consequently, salient parameters associated with the 90 deg Gurney flaps are presented as a function of $\sqrt{(h/c)}$ in Fig. 7. As may be seen, the presented parameters do indeed show a linear dependency on the square root of the flap length. In all instances, the maximum lift coefficient increases with flap length for those evaluated, with little indicated sensitivity to Re for the range shown. The minimum drag coefficient decreases with the Re increase, as may be expected. The linear dependency of the minimum drag coefficient on $\sqrt{(h/c)}$ suggests that the drag increase with flap length is due to pressure drag on the flap. The disparate slopes of the regression lines for the minimum drag coefficient also indicate a greater sensitivity to flap length changes at the lower Re (60,000). The maximum lift-to-drag ratio is also seen to increase with Re, with the higher Re data showing larger relative L/D increments when compared with the flap length increase than at $Re = 60,000$. This is likely a consequence of the reduced sensitivity of the drag coefficient to increasing flap length at higher Re. Similar trends are seen for the endurance parameter.

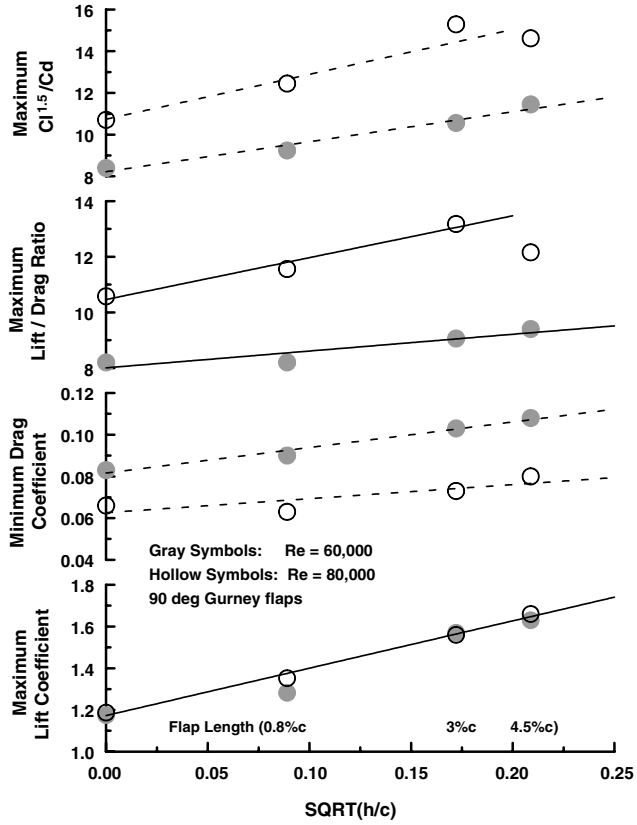

Fig. 7 Data summary showing effect of Gurney flap height on measured parameters.

Surface pressure measurement allows for the decomposition of the upper- and lower-surface loading, such that the contribution of each surface to the total lift of the airfoil may be examined. Figure 8 contains the calculated upper- and lower-surface contributions to the total lift for the clean airfoil and that with the 4.5% chord Gurney expressed as a percentage and denoted as the load ratio. Consequently, the sum of the lower and upper-surface contributions equal 100%. As may be seen at $Re = 60,000$, for an incidence range of 4 to 12 deg, the Gurney-flap-equipped airfoil shows little variation of the load division between the upper and lower surfaces; the upper surface is seen to contribute approximately 80% of the lift, while the lower surface contributes about 20%. A similar trend is seen at $Re = 80,000$. The clean airfoil at AOA $= 4$ deg shows the upper surface produces about 120% of the airfoil's lift, while the lower surface tends to suck the airfoil down, reducing lift by 20%. At 8 deg incidence, both surfaces of the clean airfoil contribute toward lift, although the lower-surface contribution is only about 10%. At 12 deg incidence, the upper surface again produces all the lift, while the lower surface produces a small negative contribution. The lower-surface pressure traces in Fig. 4b indicate the lower-surface negative lift contribution comes primarily from the aft section due to flow acceleration. At $Re = 80,000$, the clean airfoil's lower surface produces up to 20% of the total lift at AOA $= 12$ deg (see Fig. 8).

Table 2 Summary of Re and Gurney flap length effect on range and endurance parameters

	$Re = 60,000$		$Re = 80,000$	
Geometry	L/D max	$Cl^{1.5}/Cd$ max	L/D max	$Cl^{1.5}/Cd$ max
Clean	8.20	8.39	10.58	10.71
Gurney: 0.8% c	8.21	9.25	11.56	12.45
Gurney: 3% c	9.06	10.56	13.18	15.29
Gurney: 4.5% c	9.41	11.45	12.16	14.62
Gurney: 3.9% c proj., 45 deg angle	9.03	10.33	11.17	12.71

The pressure traces in Fig. 4c show that lower-surface pressures are primarily positive over the chord for the clean airfoil. The lower two insets in Fig. 8 suggest a Re dependency for the clean airfoils load devolution but not for the Gurney-flapped airfoils (for the Re range tested). This may be due to the disparate boundary-layer thickness over the lower surface at the two Re numbers (i.e., at $Re = 60,000$, a thicker boundary layer may cause reduced pressure by altering the airfoil contour through displacement thickness effects). It may also be seen that, for a given airfoil incidence, the airfoil with the Gurney produces more of its total lift from its lower surface than the clean airfoil.

Replotting the data in the lower two figures of Fig. 8 as a function of Cl, yields the top two insets in Fig. 8. The data suggest that, for a given lift coefficient, the load distribution is similar for both airfoils (with and without flap), such that the upper and lower airfoil surfaces contribute the same proportion of the total load. This is seen to be true for both Reynolds numbers. Note that not all the data points in the lower two figures are reflected in the upper insets as the clean airfoil did not produce lift coefficients comparable to the Gurney-equipped airfoil at high incidence. This result is inconsistent with that suggested in [12], where for a given lift coefficient, it was suggested that the lower surface contributes a greater proportion of the total lift by relieving the upper surface. The discrepancy may be due to Re effects or those of airfoil geometry.

Trailing-Edge Flaps

In this section, the effects of plain trailing-edge flaps are evaluated. As different airfoils were used for the Gurney flap testing, direct numerical comparisons between the data should be avoided. Limited data are presented for $Re = 40,000$. The effect of Re and flap geometry (i.e., flap angle δf and length as a percentage of the chord; $L10\%$ indicates 10% of the chord flap length) on measured lift coefficient is presented in Fig. 9. At $Re = 40,000$ (Fig. 9a), the flap is seen to shift the zero-lift AOA in the negative direction, as well as increase the airfoil's lift-curve slope when compared with the clean airfoil. In both cases, a distinct stall is not clearly identifiable, with lift curves similar in appearance to those seen for thin flat plates. Hysteresis is seen to be marginal, due to excessive boundary-layer stability and, thus, lack of free transition. Increasing Re to 60,000 and 80,000 (Figs. 9b and 9c) shows significant performance improvement, with a clearly identifiable stall and increase in lift-curve slope. The curves at the higher Re appear less linear in the attached flow regime then at $Re = 40,000$, suggestive of the presence and movement of separation bubbles with incidence (they may not form at $Re = 40,000$). For plot clarity, hystereses data are not included at $Re = 60,000$ and 80,000. However, it was observed from the plots that, at $Re = 60,000$, the hystereses loops were generally small in magnitude excursion, while at $Re = 80,000$, the loops were larger and typically showed closure within a 2 deg incidence. Although trailing-edge flaps usually reduce the stall incidence, this is not seen to be the case for all data sets at $Re = 60,000$. At $Re = 80,000$, the 10 deg flap deflection curves for both the 10- and 20%-long flaps are seen to show stall at approximately the same incidence as the clean airfoil. At $Re = 80,000$, all other flap geometries show stall at approximately a 2 deg lower incidence than the clean airfoil (within the measurement resolution). Note that, at $Re = 60,000$, data for the 10% chord flap with a 20 deg deflection are included for consistency, but they are not deemed reliable. Surface flow patterns (not included) showed that the trailing-edge flap significantly shortened the separation bubble for a given incidence when compared with the clean airfoil without a marked alteration in the separation location. The large increase in the adverse pressure gradient associated with flaps likely contributes to enhanced shear layer disturbance amplification, yielding earlier transition.

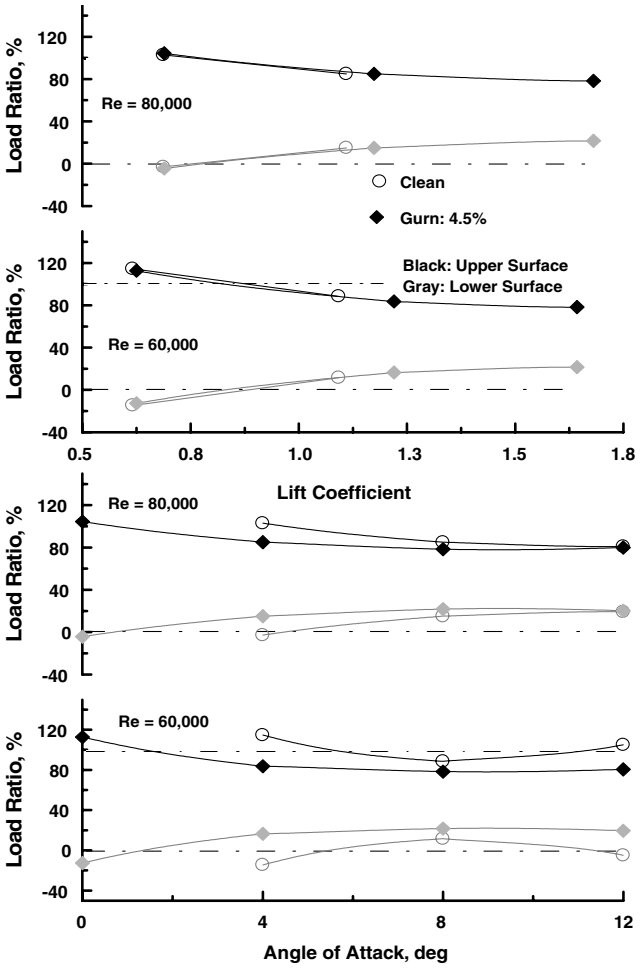

Fig. 8 Upper- and lower-surfaces load distribution.

As may be expected, increasing flap angle results in greater lift augmentation for a given incidence for both $Re = 60,000$ and 80,000, effected primarily through a shift of the zero-lift AOA. The maximum lift coefficient also increases with flap length. For a given flap setting angle and Re, the 20% chord flaps are seen to produce a greater lift increment than the 10% chord flaps.

Effects of the trailing-edge flaps on drag and the drag-based parameters L/D and $Cl^{1.5}/Cd$ are displayed in Fig. 10. Table 3 presents a summary of recorded maximum values of these parameters. Figure 10a shows the effect of the 20% chord flap with a deflection of 20 deg at $Re = 40,000$. As seen, the flap causes a moderate increase in the airfoil's minimum drag coefficient. Effects on L/D and $Cl^{1.5}/Cd$ are negligible until $Cl > 0.6$, which may be identified as the incidence at which large-scale separation manifests over the clean airfoil. As the flap significantly increases the maximum lift, peak values of L/D and $Cl^{1.5}/Cd$ are appreciably augmented. For clarity, summary plots for the $Re = 60,000$ and 80,000 have been split into flap length, such that the flap deflection angle is variable (see Figs. 10b and 10c, as well as Figs. 10d and 10e, respectively). At $Re = 60,000$, all flap settings, excluding the 10% chord flap with 10 deg deflection, show an increase in drag in the attached flow regime (Figs. 10b and 10c). Consequently, the drag-based parameters degrade for $Cl < 1$ when compared with the clean airfoil. For the 10% chord flaps, a 10 deg deflection shows a significant increase in L/D and $Cl^{1.5}/Cd$ when compared with the other configurations and clean airfoil. Increasing the flap length to 20% chord (Fig. 10c) shows an improvement in L/D and $Cl^{1.5}/Cd$ for $Cl > 1$ when compared with the clean airfoil for all flap settings. Peak recorded values are seen to be similar for both the 10 and 20 deg deflections, while the significant drag penalty of the 30 deg deflection is reflected in reduced L/D.

Boundary-layer improvement is obvious with the increase in Re to 80,000 (see Figs. 10d and 10e). The drag penalty associated with flap deflection is reduced significantly and, in certain cases, is not present. For the 10% chord flaps (Fig. 10d), they either match or exceed L/D and $Cl^{1.5}/Cd$ for $Cl < 0.4$ and significantly enhance these parameter for $Cl > 0.4$ when compared with the clean airfoil. Performance increases (compared to the clean airfoil) are seen to show moderate

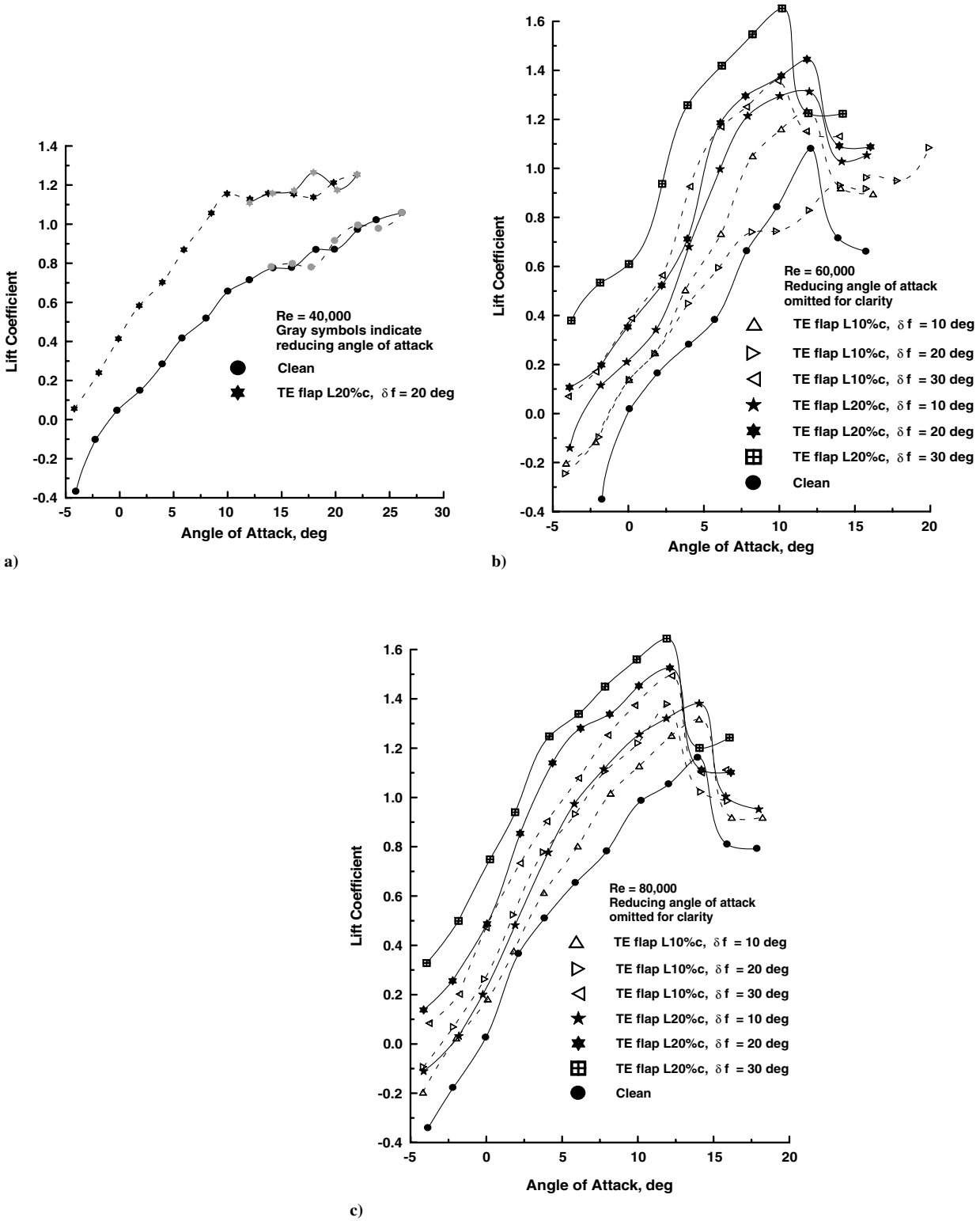

Fig. 9 Effect of Re and flap geometry on measured lift coefficient: a) $Re = 40,000$, b) $Re = 60,000$, and c) $Re = 80,000$.

sensitivity to the flap setting for the angles explored. The 20% chord flaps show a greater sensitivity to flap angle, with a deflection of 20 deg yielding the best performance (Fig. 10e). However, the large drag penalty of the 30 deg deflection causes a reduction in L/D and $Cl^{1.5}/Cd$, which is only compensated for by its enhanced lifting ability at high $Cl(>1.1)$.

Gurney and Trailing-Edge Flaps

Because of obvious differences in the minimum drag coefficients, L/D and $Cl^{1.5}/Cd$ data should not be directly compared between the Gurney and trailing-edge flap configurations. However, inferences may be drawn if differences between the flap and its respective clean airfoil baseline are investigated. Table 4 contains a summary of measured maximum lift as a function of flap geometry and Re. Both the Gurney flap and trailing-edge flap show significant maximum lift augmentation, as evidence by the percent increase (% increase) relative to the clean airfoil. For the configurations evaluated, both flow effectors are seen to be capable of similar lift increments when compared with the clean airfoil, approximately 40%. The maximum lift coefficient appears to have little sensitivity to Re for the limited range explored.

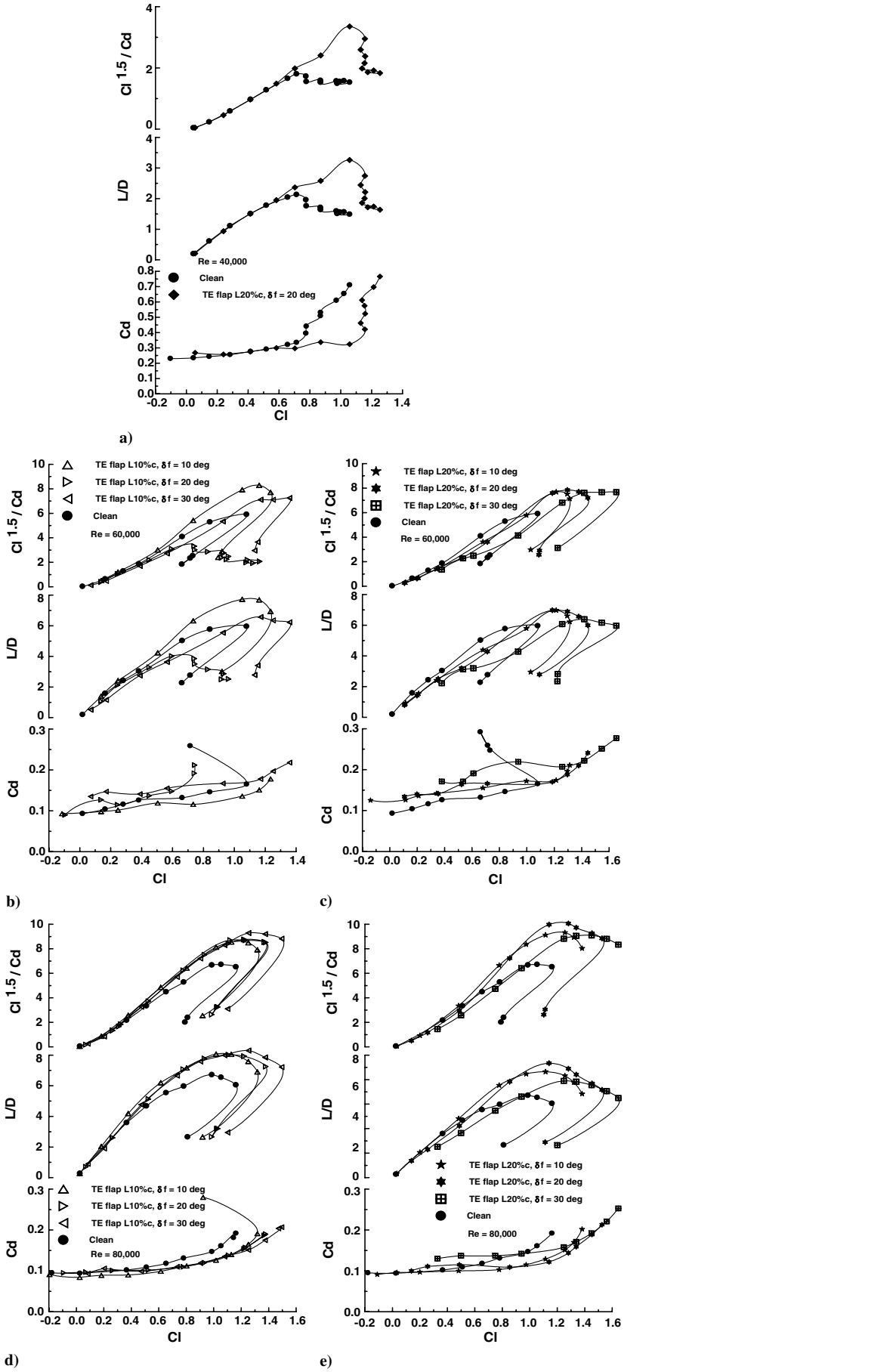

Fig. 10 Effect of *Re* and flap geometry on measured drag based parameters: a) $Re = 40,000$, 20% c flap; b) $Re = 60,000$, 10% c flap; c) $Re = 60,000$, 20% c flap; d) $Re = 80,000$, 10% c flap; and e) $Re = 80,000$, 20% c flap.

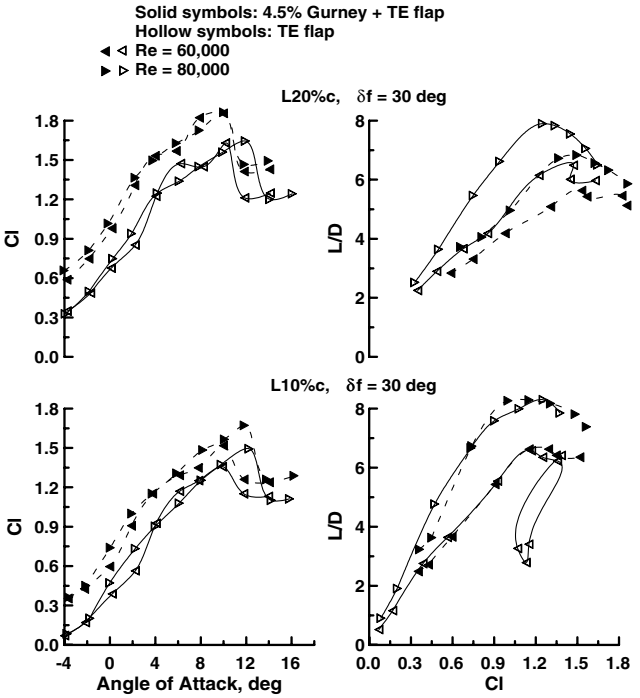

Fig. 11 Effect of 4.5% Gurney trailing-edge flap combination on measured lift coefficient and lift-to-drag ratio.

Examination of Tables 2 and 3 indicates that both flap types can improve L/D and $Cl^{1.5}/Cd$, characteristics not always associated with trailing-edge lift modulation devices at higher Re. The maximum L/D increase, when compared with the clean airfoil for the Gurney flap, is 14.8 (4.5% flap) and 24.6% (3% flap) for $Re = 60,000$ and 80,000, respectively. The trailing-edge flaps recorded a 17.1 and 39.2% (20% long, 20 deg deflection) increase for similar conditions, showing the improvement effects of Re. Maximum $Cl^{1.5}/Cd$ increases are 36.5 and 42.8% for the Gurney flap and 32.7 and 49.8% for the trailing-edge flaps for $Re = 60,000$ and 80,000, respectively. The increases in L/D and $Cl^{1.5}/Cd$ (which all occur close to the maximum lift coefficient) with flaps is seen to result primarily from the increase in maximum lift. Note that the cited results are not meant to be absolutes or optimal values but indicative of the general characteristics of the lift augmentation devices explored.

A limited study was also undertaken to establish the effect of combining the 4.5%-long Gurney flap with the trailing-edge flap. A flap deflection angle of 30 deg was used for both 10 and 20% chord flaps. Results are presented in Fig. 11. When used in conjunction with a trailing-edge flap, the Gurney is seen to negatively shift the zero-lift AOA, such that the Gurney shows a relatively constant lift increment when compared with the plain flap (an increment of approximately 0.25–0.4, depending on Re). The increment is seen to be slightly reduced when compared with that relative to the plain airfoil (Figs. 6a and 6b). With the 20% combination flap, a Cl max >1.8 is achieved, an increase of over 60% when compared to the clean airfoil (see Table 4). The impact of the combined flaps on the lift-to-drag ratio is less beneficial, with no observable improvement for the 10%-long flap combination over the plain flaps and a significant reduction in L/D for the 20%-long flap combination. Examination of the drag data showed a significant increase in the minimum drag coefficient for these combined flap cases.

Conclusions

A low-speed wind-tunnel study was undertaken to investigate the effect of trailing-edge lift augmentation devices at $Re = 40,000$, 60,000, and 80,000 on a S8036 airfoil section. Gurney flaps, as well as conventional plain trailing-edge flaps, were investigated. The effect of Gurney flap length was evaluated, as well as trailing-edge flap length and deflection angle. Data presentation encompassed force balance and pressure measurements. The data showed that both the Gurney and trailing-edge flaps can significantly increase the maximum lift coefficient, with increases of 40% recorded. The

Table 3 Summary of *Re* and trailing-edge flap geometry effects on range and endurance parameters

	$Re = 60,000$		$Re = 80,000$	
Geometry	L/D max	$Cl^{1.5}/Cd$ max	L/D max	$Cl^{1.5}/Cd$ max
Clean, $\delta f = 0$ deg	5.96	5.91	6.71	6.72
TE flap $L10\%c$, $\delta f = 10$ deg	7.72	8.28	8.07	8.56
TE flap $L10\%c$, $\delta f = 20$ deg	4.02[a]	3.32[a]	8.02	8.76
TE flap $L10\%c$, $\delta f = 30$ deg	6.57	7.11	8.30	9.29
TE flap $L20\%c$, $\delta f = 10$ deg	6.98	7.69	8.64	9.32
TE flap $L20\%c$, $\delta f = 20$ deg	6.98	7.84	9.34	10.07
TE flap $L20\%c$, $\delta f = 30$ deg	6.34	7.67	7.90	9.09

[a]Data nonrepresentative.

Table 4 Effect of Gurney flap length and trailing-edge flap geometry on measured maximum lift coefficient

	$Re = 60,000$		$Re = 80,000$	
Geometry	Cl maximum	% increase	Cl maximum	% increase
Clean	1.18	–	1.19	–
Gurney: 0.8%	1.28	8.5	1.35	13.5
Gurney: 3%	1.57	33.1	1.56	31.1
Gurney: 4.5%	1.63	38.1	1.66	39.5
Gurney: 3.9% proj., 45 deg angle	1.43	21.2	1.49	25.2
Clean, $\delta f = 0$ deg	1.1	——	1.16	——
TE flap $L10\%c$, $\delta f = 10$ deg	1.24	12.7	1.32	13.8
TE flap $L10\%c$, $\delta f = 20$ deg	1.16	5.5	1.38	18.9
TE flap $L10\%c$, $\delta f = 30$ deg	1.36	23.6	1.49	28.5
TE flap $L20\%c$, $\delta f = 10$ deg	1.31	19.1	1.38	18.9
TE flap $L20\%c$, $\delta f = 20$ deg	1.45	31.8	1.53	31.9
TE flap $L20\%c$, $\delta f = 30$ deg	1.65	50.0	1.65	42.2

Reynolds number did not appear to significantly affect the lift increase for the range explored. Increasing the Gurney flap length generally improved performance for the flap lengths investigated (up to 4.5% chord), a result of the large boundary-layer thickness present at low Re. The Gurney flap increases lift though a negative zero-lift shift, in combination with an increase of lift-curve slope. Examination of upper- and lower-surface pressure traces showed that the Gurney flap caused increased loading on the lower surface when compared with an unmodified airfoil; however, based on an equal lift comparison, the load distribution or split between the upper and lower surfaces appears similar for the Gurney modified and clean airfoils. Defining Gurney flap parameters, such as the maximum lift and minimum drag coefficient, as well as the range and endurance parameters, was seen to show a strong correlation with the square root of the flap length. Examination of trailing-edge flap lift augmentation indicated that the smallest explored angle, 10 deg, was the most efficient for both flap lengths. For a similar deflection angle, the 20%-long flap showed greater lift increments than the 10%-long flap.

Both the Gurney flap and trailing-edge flaps showed a significant increase in the maximum lift-to-drag ratio, as well as $Cl^{1.5}/Cd$, when compared with the clean airfoil. Increases in the minimum drag coefficient with either a trailing-edge or Gurney flap were reflected in a reduction in L/D and $Cl^{1.5}/Cd$ at low lift coefficients when compared with the clean airfoil. The effect of flap length was not clearly definable at $Re = 60,000$ on L/D and $Cl^{1.5}/Cd$; at $Re = 80,000$, the longer 20% flap showed greater performance augmentation. A combination of the Gurney flap with the trailing-edge flap showed additional lift enhancement coupled with a reduction in lift-to-drag performance.

Acknowledgement

The authors would like to thank the associate editor and reviewers for their comments and suggestions.

References

[1] Mueller, T. J., "Aerodynamic Measurements at Low Reynolds Numbers for Fixed Wing Micro-Air Vehicles," *RTO AVT/VKI Course*, von Karman Inst., Belgium, 13 Sept. 1999.

[2] Mueller, T. J., "The Influence of Laminar Separation and Transition on Low Reynolds Number Airfoil Hysteresis," *Journal of Aircraft*, Vol. 22, No. 9, 1985, pp. 763–770. doi:10.2514/3.45199

[3] Perry, M. L., and Mueller, T. J., "Leading and Trailing Edge Flaps on a Low Reynolds Number Airfoil," *Journal of Aircraft*, Vol. 24, No. 9, 1987, pp. 653–659. doi:10.2514/3.45491

[4] Lissaman, P. B. S., "Low-Reynolds-Number Airfoils," *Annual Review of Fluid Mechanics*, Vol. 15, No. 1, 1983, pp. 223–239. doi:10.1146/annurev.fl.15.010183.001255

[5] Traub, L. W., and Cooper, E., "Experimental Investigation of Pressure Measurement and Airfoil Characteristics at Low Reynolds Numbers," *Journal of Aircraft*, Vol. 45, No. 4, 2008, pp. 1322–1333. doi:10.2514/1.34769

[6] Weick, F. E., and Shortal, J. A., "The Effect of Multiple Fixed Slots and a Trailing Edge Flap on the Lift and Drag of a Clark Y Airfoil," NACA Rept. 427, April 1932.

[7] Jeffrey, D. R., and Hurst, D., "Aerodynamics of the Gurney Flap," AIAA Paper 96-2418, 1996.

[8] Zerihan, J., and Zhang, X., "Aerodynamics of Gurney Flaps on a Wing in Ground Effect," *Journal of Aircraft*, Vol. 39, No. 5, 2001, pp. 772–780. doi:10.2514/2.1396

[9] Maughmer, M. D., and Bramesfeld, G., "Experimental Investigation of Gurney Flaps," *Journal of Aircraft*, Vol. 45, No. 6, 2008, pp. 2062–2067. doi:10.2514/1.37050

[10] Bearman, P. W., "On Vortex Street Wakes," *Journal of Fluid Mechanics*, Vol. 28, No. 4, 1967, pp. 625–641. doi:10.1017/S0022112067002368

[11] Cavanaugh, M., Robertson, P., and Mason, W. H., "Wind Tunnel Test of Gurney Flaps and T-Strips on an NACA 23012 Wing," AIAA Paper 2007-4175, June 2007.

[12] Meyer, R., Hage, W., Bechert, D. W., Schatz, M., and Thiele, F., "Drag Reduction on Gurney Flaps by Three Dimensional Modifications," *Journal of Aircraft*, Vol. 43, No. 1, 2006, pp. 132–140. doi:10.2514/1.14294

[13] Mayda, E. A., van Dam, C. P., and Nakafuji, "Computational Investigation of Finite Width Microtabs for Aerodynamic Load Control," AIAA Paper 2005-1185, 2005.

[14] Lee, T., "Aerodynamic Characteristics of Airfoil with Perforated Gurney Type Flaps," *Journal of Aircraft*, Vol. 46, No. 2, 2009, pp. 542–548. doi:10.2514/1.38474

[15] Traub, L. W., Miller, A. C., and Rediniotis, O., "Preliminary Parametric Study of Gurney Flap Dependencies," *Journal of Aircraft*, Vol. 43, No. 4, 2006, pp. 1242–1244. doi:10.2514/1.13852

[16] Yarusevch, S., Kawall, J. G., and Sullivan, P. E., "Separated-Shear-Layer Development on an Airfoil at Low Reynolds Numbers," *AIAA Journal*, Vol. 46, No. 12, 2008, pp. 3060–3069. doi:10.2514/1.36620

[17] Smith, A. M. O., "High-Lift Aerodynamics," *Journal of Aircraft*, Vol. 12, No. 6, 1975, pp. 501–530. doi:10.2514/3.59830

[18] Kuethe, A. M., and Chow, C., *Foundations of Aerodynamics*, 4th ed., Wiley, New York, 1986, pp. 413–417.

[19] Traub, L. W., "Effects of Gurney Flaps on an Annular Wing," *Journal of Aircraft*, Vol. 46, No. 3, 2009, pp. 1085–1088. doi:10.2514/1.43096

[20] Liu, T., and Montefort, J., "Thin-Airfoil Theoretical Interpretation for Gurney Flap Lift Enhancement," *Journal of Aircraft*, Vol. 44, No. 2, 2007, pp. 667–671. doi:10.2514/1.27680